

## Functionalization of ceramic tile surface by soluble salts addition: Part II. Titanium and silver addition

Federica Bondioli<sup>a,\*</sup>, Martina Dinelli<sup>a</sup>, Roberto Giovanardi<sup>a</sup>, Michele Giorgi<sup>b</sup>

<sup>a</sup> *Università di Modena e Reggio Emilia, Dipartimento di Ingegneria dei Materiali e dell'Ambiente, Via Vignolese 905, 41100 Modena, Italy*

<sup>b</sup> *METCO srl, Via Galileo Galilei 53, Monteveglio, BO, Italy*

Received 24 September 2009; received in revised form 25 February 2010; accepted 17 March 2010

### Abstract

The aim of this study was to assess surface functionalization of industrial ceramic tiles through the addition of soluble salts to improve mechanical properties (scratch and wear resistance) and conductivity, while preserving the aesthetic aspects of the finished product. This objective was pursued through the application of different solutions of titanium and silver with a potential for transformation into titania and silver nanoparticles during the sintering of the material. The solutions, in different concentrations, were applied (300 g/m<sup>2</sup>) to unglazed green tiles by air brushing. The resulting products were polished and characterized in terms of microstructural, surface micromechanical, and technological properties based on the UNI EN ISO reference standards. The electrical conductivity deriving from the presence of titania and silver was also established with specific tests. The results were found to correlate with the results obtained from the addition of zirconium solutions as reported in part I of the paper. Crown Copyright © 2010 Published by Elsevier Ltd. All rights reserved.

**Keywords:** Functionalization; Tile; Silver; Titania; Scratch resistance; Antistatic floor

### 1. Introduction

The development of advanced materials, mainly intended to improve the shapes and mechanical characteristics of structures, is increasingly leading to integration of functions into materials and components. This drive in technological innovation is strongly felt in many traditional fields, like textiles or ceramics. Over the last 20 years, the so-called “traditional” ceramics industry for tile production has undergone a profound technological reorganization, both in production technologies and the automation of the different production phases, but new products and possible new applications are still needed, thereby opening up new markets. As a contribution to this innovative process the authors are proposing continuous evolution of the aesthetics and functionality of products. The work described in this paper is part of a wider project focused on the surface functionalization of industrial tiles. This aim is pursued through the design and preparation of nanostructured powders, and innovative technologies for the creation of nanostructured materials.

The development of functionalized surfaces has recently been focused on in nanotechnology, for example, investigating self-cleaning surface using TiO<sub>2</sub> nanoparticles.<sup>1–5</sup> In a recent work, the authors reported the possibility of tile surface functionalization using a sol–gel technique to improve both wear resistance and cleanliness of unglazed surfaces.<sup>6</sup> A TiO<sub>2</sub>–SiO<sub>2</sub> binary film was deposited on fired tiles by air brushing to obtain a photocatalytically active building material, a self-cleaning and self-sterilizing surface that could also degrade several organic contaminants in the surrounding environment by UV radiation activation. Moreover, in part I of this work,<sup>7</sup> the authors showed that the addition of zirconium soluble salts offered an increase in scratch resistance, while maintaining the final aesthetic appearance of the resulting tiles. Part II (the present text) assesses the effects of application of different titanium and silver solutions, which can be transformed into titania and silver nanoparticles during the sintering of the material. The idea is to exploit the transparency of nanoparticles to obtain a multifunctional surface with a higher degree of sintering than the ceramic body. In addition to the improved mechanical properties expected from the addition of titania, silver solutions were tested to evaluate the possibility of obtaining antistatic materials for flooring in industry, offices, hospitals, computer rooms, etc. The presence

\* Corresponding author. Tel.: +39 059 205 6242; fax: +39 059 205 6243.  
E-mail address: [federica.bondioli@unimore.it](mailto:federica.bondioli@unimore.it) (F. Bondioli).

Table 1  
Chemical composition of the prepared solutions.

Sample	Ti content (ppm)	Sample	Ti content (ppm)	Ag content (ppm)	Sample	Ti content (ppm)	Ag content (ppm)
Ti1	12.8	10TiAg1	9.40	0.94	5TiAg1	4.70	0.94
Ti2	25.6	10TiAg2	18.8	1.88	5TiAg2	9.40	1.88
Ti3	51.3	10TiAg3	37.5	3.75	5TiAg3	18.8	3.75
Ti4	103	10TiAg4	75.0	7.50	5TiAg4	37.5	7.50
Ti5	205	10TiAg5	150	15.0	5TiAg5	75.0	15.0
Ti6	410	10TiAg6	300	30.0	5TiAg6	150	30.0

of conductive nanoparticles in the matrix enables the formation of low resistance paths that could reduce both the surface and volume resistivity of the tiles.<sup>8,9</sup> Titanium-based solutions with different silver contents were applied by air brushing to ceramic tiles before sintering. The solutions, in different concentrations, were deposited (300 g/m<sup>2</sup>) on unglazed green tiles. After an industrial thermal treatment, the resulting products were polished and characterized in terms of microstructural, surface micromechanical, and technological properties based on the UNI EN ISO reference standards. Electrical conductivity due to the presence of silver was also determined with specific tests. The antistatic behavior of the resulting tiles was evaluated using the dimensionless resistivity ( $\chi$ ) approach introduced by Oshawa.<sup>10</sup> The final aesthetic appearance and hue variations of the products were evaluated by vis–UV spectroscopy and colorimetric analysis<sup>11,12</sup>.

## 2. Experimental

The solutions were specially prepared by METCO Srl. and referenced as reported in Table 1. The application of 300 g/m<sup>2</sup> of solution was performed as reported in part I.<sup>7</sup> After this treatment, the compounds were dried at 105 °C to a constant weight and then fired in a semi-industrial kiln at  $T_{\max}$  1210 °C in a 60 min cycle. All the fired samples were also polished in order to obtain mirror-finish surfaces, removing 0.5 mm of the surface layer.

The effect of the addition of titanium and silver on the esthetic (color and gloss), mechanical (scratch test), and technological properties of the resulting tiles was assessed as reported in part I.<sup>7</sup>

The electrical properties of the coated ceramic tiles were tested by measuring their volume resistivity ( $\rho_v$ ) and surface

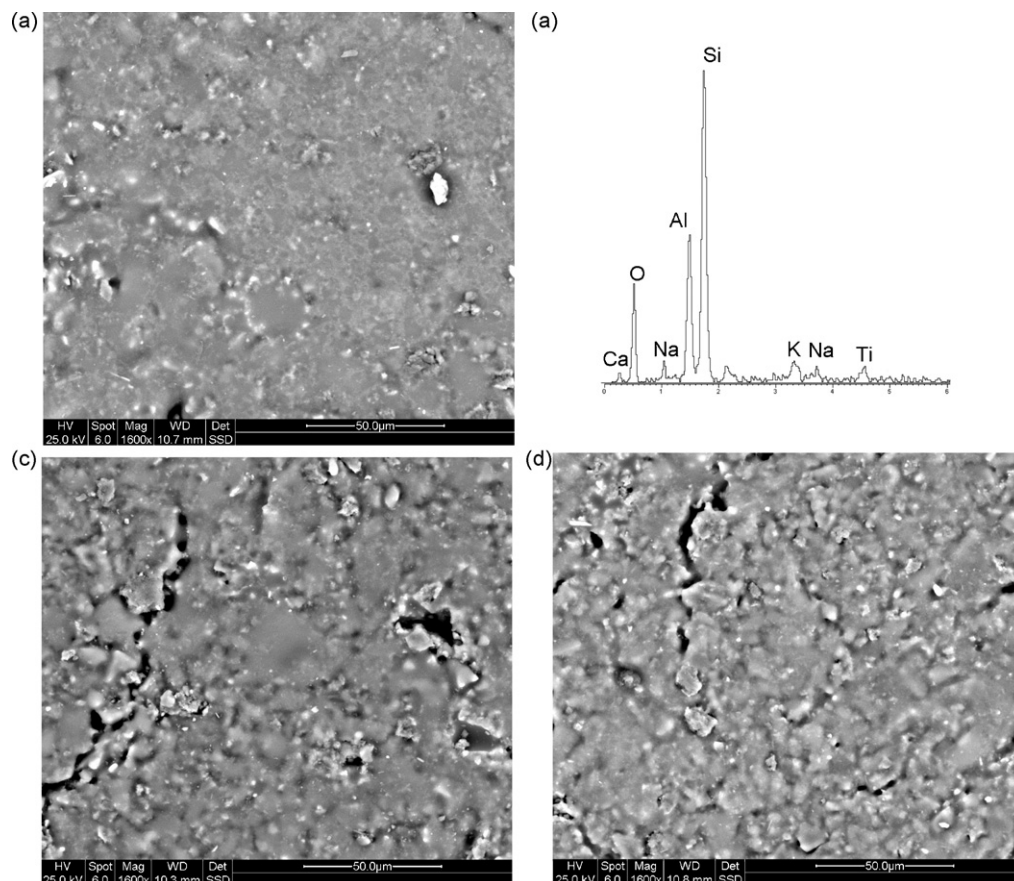


Fig. 1. SEM micrographs of the Ti6 (a), Ti1 (c), and untreated tile (d) surfaces. EDS spectra (b) of white crystals in the Ti6 sample.

Table 2

 $\Delta E^*$  and gloss values of the prepared coatings.

Sample code	Gloss (GU)	$\Delta E^*$	Sample code	Gloss (GU)	$\Delta E^*$	Sample code	Gloss (GU)	$\Delta E^*$
Ti1	4.4	0.53	10TiAg1	4.2	0.79	5TiAg1	4.2	0.45
Ti2	4.4	0.56	10TiAg2	4.2	0.58	5TiAg2	4.6	0.50
Ti3	4.5	0.28	10TiAg3	4.0	1.14	5TiAg3	4.3	0.70
Ti4	4.8	0.56	10TiAg4	4.5	0.87	5TiAg4	4.7	0.43
Ti5	4.9	0.53	10TiAg5	4.9	1.62	5TiAg5	5.4	1.11
Ti6	4.3	1.93	10TiAg6	5.2	2.36	5TiAg6	5.0	0.98

resistivity ( $\rho_s$ ) using an electrometer (model 6517A Keithley) connected to a resistivity test chamber (model 8009 Keithley). To avoid polarization of the ceramic material and dielectric separation phenomena during volume resistivity ( $\rho_v$ ) measurements, a method based on alternate polarity was used: the electric potential was alternated regularly and instantaneously between two levels (+500 V, −500 V) maintaining each level constant for 3 min and producing a square wave. At the end of each constant potential period the value of the current was recorded and the sample resistance calculated. The test is completed when six measurements have been performed and, using the arithmetic average value of resistance, the volume resistivity value was calculated according to Ohm's Second Law.

Surface resistivity ( $\rho_s$ ) was measured applying a polarization of +1000 V between the guarded electrode and the ring electrode of the test chamber.

Before resistivity measurements, the ceramic samples were kept in a climatic chamber for 24 h (model M120, RH Instruments) at a temperature of 25 °C and relative humidity of 50%. The temperature and relative humidity were selected as the closest to ambient conditions. This procedure avoids water absorption or desorption phenomena in the ceramic tiles during measurements, which greatly influence this type of data.

The volume resistivity values ( $\rho_v$ ) and the surface resistivity values ( $\rho_s$ ) reported in the present work are the average value of three different measurements, repeated as described before.

The results were correlated with diffractometric and microstructural analysis data obtained as reported in part I.<sup>7</sup>

### 3. Results and discussion

The linear shrinkage (LS%) and water absorption (WA%) results assure that the proposed treatment is compatible with industrial production. Water absorption significantly decreases (from 0.28 to 0.12%) as the titanium concentration is increased compared to commercial materials (0.33%) suggesting a higher degree of sintering of the products. This is supported by the microstructural analysis of the surfaces (Fig. 1), which showed that the Ti6 sample, with the highest titanium concentration, had a higher compaction, while the Ti1 sample had a surface comparable with that of untreated tiles. Moreover, the images clearly showed that the presence of white crystals, attributable to titania phase as underlined by the EDS spectra, decreases as the titanium content in solution is decreased (Fig. 1a and c). The same behavior is observed when silver is added to the titanium solution.

Aesthetic results (expressed by  $\Delta E^*$  between the treated tile surfaces and the untreated tile surface and gloss<sup>11,12</sup>) are reported in Table 2. In general the  $\Delta E^*$  values are <1, indicating that there is not a visible hue variation due to the application of the solutions compared to the untreated tile. This result indicates that the titania nanoparticles are well dispersed in the matrix. A different behavior is observed in the samples with a higher titanium content (Ti6, 10TiAg5, 10TiAg6, 5TiAg5, and 5TiAg6) where the  $\Delta E^*$  values are higher than 1. These values can be correlated with the microstructural analysis, which showed higher crystal concentrations on the surfaces.

All the samples exhibit a gloss parameter comparable to that of the untreated surface (4.40 GU) indicating that the deposited solutions do not significantly modify the roughness of the samples, in agreement with the images reported in Fig. 1.

As in part I,<sup>7</sup> the crystalline phases developed by the soluble salts were qualitatively characterized by X-ray diffraction measurements (XRD), as shown in Fig. 2. From the XRD results it is reasonable to assume that, during the sintering stage, titania crystallized as rutile (ICDD #00-001-1292). The presence of rutile is compatible with the tile sintering temperature, rutile being the stable phase at high temperatures. Particular attention was dedicated to the XRD patterns obtained on samples also treated with Ag, where there is no evidence of any phase containing silver. This result suggests the possible dissolution of the Ag ion in the glassy phase developed, during the sintering stage, from the feldspars.

To assess the effect of the proposed treatment on mechanical properties, scratch tests with linearly increasing loads were performed on the samples. The critical load values for both pol-

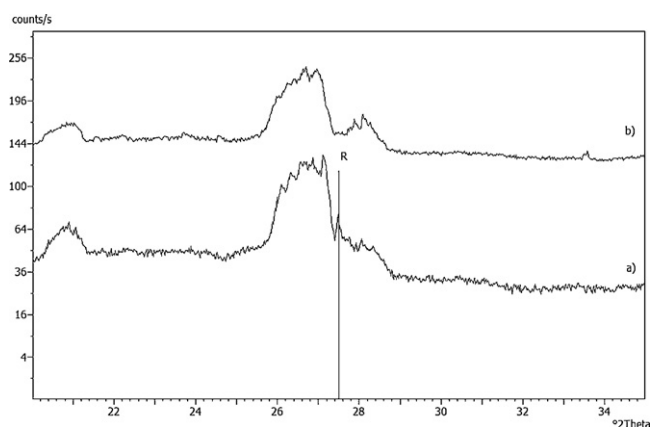


Fig. 2. XRD patterns of the Ti5 sample (a) compared with the untreated sample (b). R = rutile.

Table 3  
Critical loads  $L_{C2}$  of samples<sup>a</sup>.

Sample code	$L_{C2}$ (N)		Sample code	$L_{C2}$ (N)		Sample code	$L_{C2}$ (N)	
	Unpolished	Polished		Unpolished	Polished		Unpolished	Polished
Uncoated tile	7.84 ± 0.56	7.74 ± 0.01						
Ti1	12.34 ± 0.63	10.42 ± 0.92	10TiAg1	7.89 ± 1.71	9.73 ± 1.15	5TiAg1	7.34 ± 0.86	8.23 ± 1.90
Ti2	12.33 ± 1.50	10.75 ± 1.13	10TiAg2	8.74 ± 1.42	9.41 ± 1.32	5TiAg2	7.98 ± 1.56	8.44 ± 1.87
Ti3	12.32 ± 1.73	12.10 ± 1.05	10TiAg3	9.52 ± 0.70	10.32 ± 1.85	5TiAg3	8.47 ± 1.65	9.92 ± 1.05
Ti4	12.29 ± 1.81	12.51 ± 1.53	10TiAg4	10.74 ± 1.90	10.41 ± 1.56	5TiAg4	9.39 ± 1.56	9.30 ± 0.26
Ti5	13.82 ± 1.36	10.53 ± 1.10	10TiAg5	10.32 ± 1.76	9.82 ± 0.21	5TiAg5	9.87 ± 0.96	8.20 ± 1.59
Ti6	14.02 ± 1.37	10.50 ± 0.77	10TiAg6	13.08 ± 1.88	9.19 ± 1.73	5TiAg6	12.08 ± 1.72	8.27 ± 1.17

<sup>a</sup> Only the  $L_{C2}$  values were reported because the surfaces roughness did not allow the determination of  $L_{C1}$  values.

ished and unpolished samples are reported in Table 3. As regards the unpolished tiles, all the treated samples exhibited higher  $L_{C2}$  values compared to the untreated sample (7.8 N). Moreover, as the dilution is increased,  $L_{C2}$  decreases, indicating a direct correlation with the superficial mechanical properties. In fact, a higher dilution involves both a lower metal content and a higher penetration of the solutions into the ceramic bodies, which means that the nanoparticles are not only fewer, but also more dispersed in the matrix. In particular, the Ti5 and Ti6 samples have the highest values (13.8 and 14 N, respectively) with an increase of almost 44% compared to the untreated sample. Finally, the addition of silver leads to a slight modification of the  $L_{C2}$  values, with the TiX samples exhibiting higher values compared with the 10TiAgX and 5TiAgX samples. Regarding the polished samples, the table highlights a different behavior for Ti concentration. The  $L_{C2}$  values initially increase as the dilution is increased and, in general, reach the maximum value for the X3 and X4 samples. During the polishing stage 0.5 mm of the superficial layer is removed and, consequently, in the samples characterized by lower penetration and higher titanium concentration the titania particles are also removed. Again, the TiX samples have higher values compared with the 10TiAgX and 5TiAgX samples. Finally, the Ti3 and Ti4 samples have the highest  $L_{C2}$  value (12 N), increased 36% compared to the untreated polished sample (7.7 N).

The results obtained also correlate with those from the application of zirconium solutions.<sup>7</sup> In general the increase of  $L_{C2}$  achieved by the addition of titanium is higher, especially in the unpolished samples. The zirconium solution produced a maximum increase of 22%. On the contrary, for the polished sample, the percentage increase is almost the same. This outcome is due to the higher metal content in the initial solution of the Ti-based solutions.

Fig. 3 shows the volume resistivity values for the unpolished ceramic tiles. The treated samples were compared to an untreated one, a reference sample identified in each graph by a star symbol. All the treated samples had higher conductivity (lower  $\rho_v$ ) compared with the untreated one. The most marked increase was obtained using the 5TiAg solution, with a higher content of Ag. These results suggest that, as expected (at temperatures higher than 500 K the metallic phase is thermodynamically stable for silver<sup>13,14</sup>), the addition of Ag is relevant for enhancing the conductivity of the sample ( $\rho_v$  reduction). Moreover it is interesting to observe the resistivity trend for TiX samples (con-

taining only Ti). Surprisingly, treatment with low concentration titanium solutions enhanced the conductivity of the samples. This can be explained in that the diluted solution has a higher degree of penetration and thus the formation of conductive titanium suboxides<sup>8</sup> in the ceramic matrix can be hypothesized during the sintering process, or, at least the formation of non-stoichiometric titanium oxide where many oxygen vacancies are present.<sup>9</sup> As the Ti concentration was increased the resistivity rose, and the sample treated with the most concentrated solution achieved a resistivity value higher than the reference (untreated sample). This can be explained in that the concentrated solution penetrates less into the ceramic tile and thus crystallizes highly resistive  $TiO_2$  particles ( $\rho_v$   $TiO_2$  between  $10^{13}$  and  $10^{18} \Omega \text{ cm}$  at 25 °C<sup>15</sup>) on the surface, as confirmed by SEM-EDS analysis (Fig. 1).

The hypotheses formulated to explain the  $\rho_v$  graph (Fig. 3) were validated by the surface resistivity results from the unpolished samples (Fig. 4). Since the surface resistivity  $\rho_s$  of samples with lower Ti concentration is comparable with that of the untreated sample, it is reasonable to assume that the less concentrated solutions penetrate deeper into the tiles, leaving a negligible quantity of silver and titania on the surface. As the titanium concentration is increased, the degree of penetration decreases explaining the increase in surface resistivity  $\rho_s$  due to a higher concentration of highly resistive  $TiO_2$  particles. Unfortunately the cross-sectional analysis performed by SEM to support

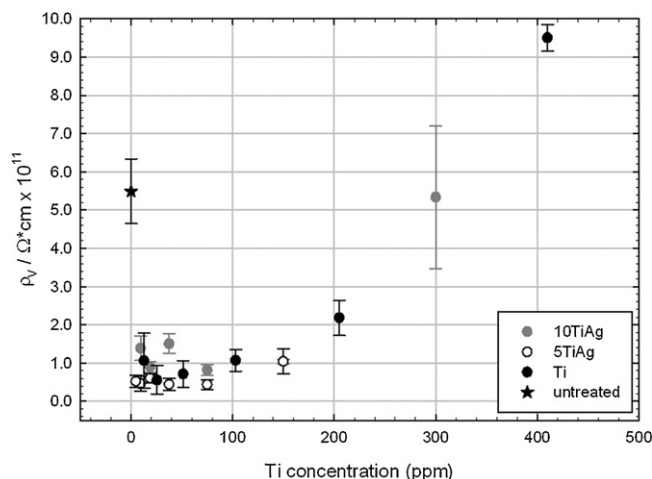


Fig. 3. Volume resistivity of the unpolished samples.



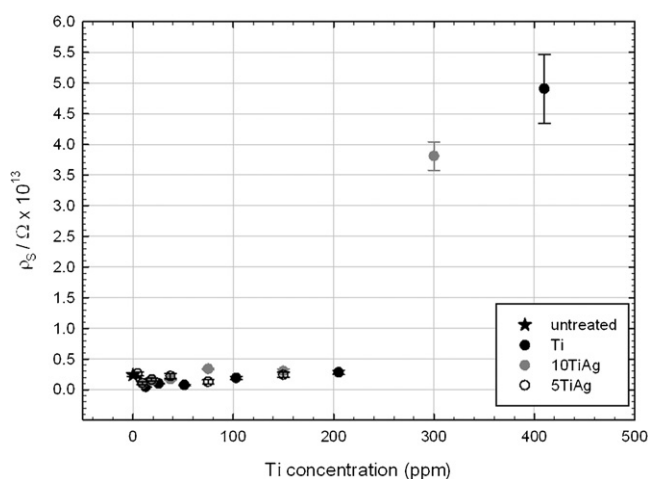


Fig. 4. Surface resistivity of the unpolished samples.

these hypotheses was not able to verify the different penetration depths in the ceramic matrix, probably due to both the low concentration of the nanoparticles and their size.

A relation between  $\rho_v$  and  $\rho_s$  to describe how their values can influence the antistatic behavior of tiles is reported by Oshawa.<sup>10</sup> He introduces dimensionless resistivity  $\chi$ , defined as:

$$\chi = \frac{\rho_s L^2}{\rho_v \delta} \quad (1)$$

where  $L$  is the length of the tiles (or the floor), considered as square shaped, and  $\delta$  is the thickness. High  $\chi$  values, from low  $\rho_v$  and high  $\rho_s$ , indicate a tendency to discharge to ground instead of dissipating the charge along the surface. Oshawa designates  $\chi$  values between  $10^{-1}$  and  $10^6$  in order to classify a floor as antistatic.

The plot in Fig. 5 is generated with the values obtained from the Oshawa formula with  $L = 10$  cm and  $\delta = 4$  mm. All the values obtained are in the range recommended by Oshawa. All the treatments lead to an increase of  $\chi$  and the higher  $\chi$  values are from the solutions containing Ag.

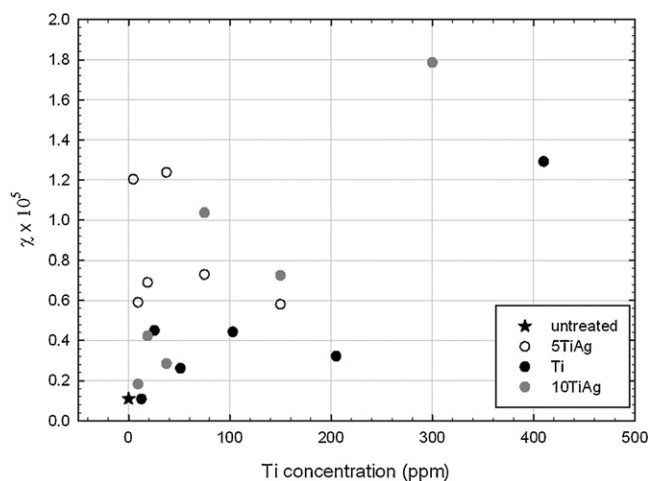
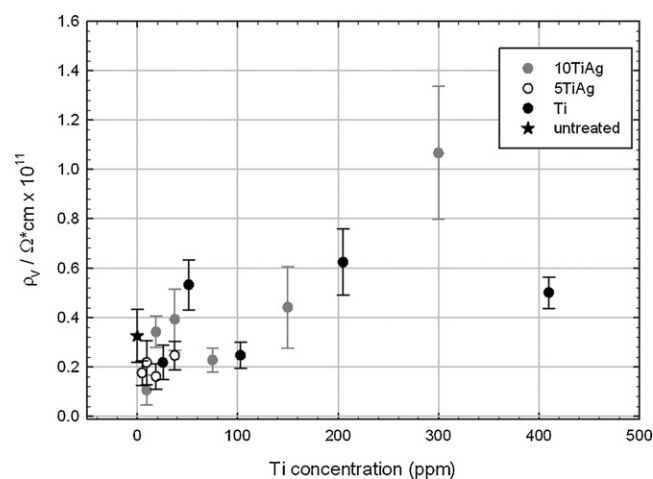
Fig. 5. Dimensionless resistivity  $\chi$  of the unpolished samples.

Fig. 6. Volume resistivity of the polished samples.

In Figs. 6 and 7 the  $\rho_v$  and  $\rho_s$  values are plotted respectively from the polished samples. Comparing these data with the unpolished tile data described in Figs. 3 and 4, it is clear how both the resistivity  $\rho_v$  and  $\rho_s$  greatly decrease after polishing. It is important to note that this effect is also observable for the reference sample, the untreated tile: this behavior can be explained by assuming that the polishing process generates a greater real surface on the sample, decreasing  $R$  and  $\rho_v$ . Polishing removes roughness, allowing closer contact between the sample and the conductive rubber of the test chamber: the result is a much larger effective contact surface. The same effect is also obvious for the  $\rho_s$  values, but in this case it is because the polishing treatment increases the superficial open porosity.

Since the  $\chi$  values are derived from the  $\rho_s$  and  $\rho_v$  ratio, the effect due to the variation in the real contact area between the sample and the conductive rubber is eliminated. This is demonstrated by comparing the  $\chi$  value of the polished reference sample and that of the corresponding unpolished sample ( $1.28 \times 10^4$  and  $1.10 \times 10^4$ , respectively).

The use of the  $\chi$  data facilitates some observations regarding the antistatic behavior of the ceramic tiles, in agreement with Oshawa: the  $\chi$  graphs greatly enhance differences, not

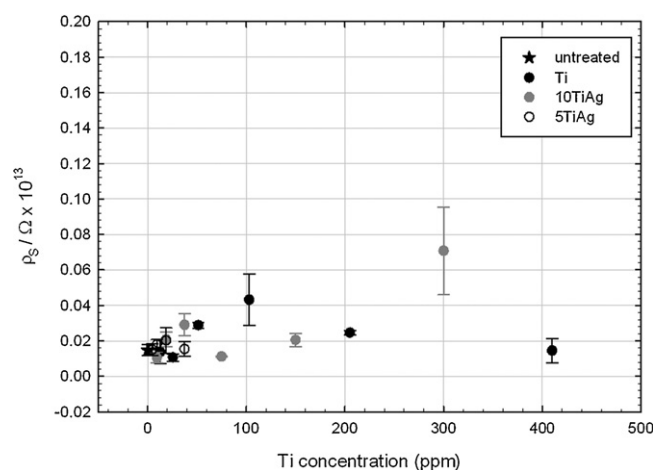


Fig. 7. Surface resistivity of the polished samples.

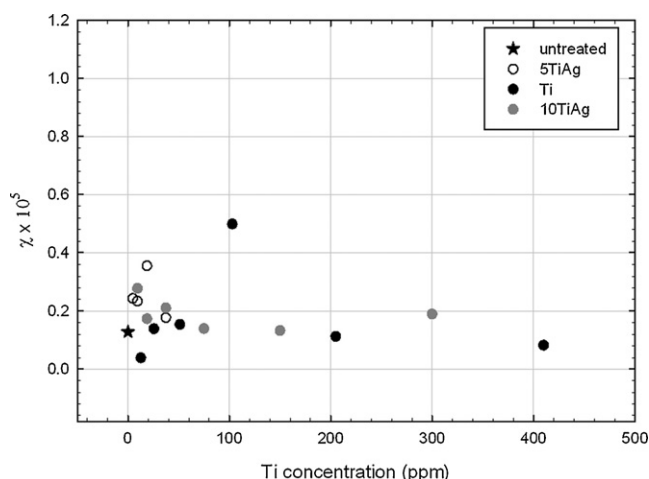


Fig. 8. Dimensionless resistivity of the polished samples.

easily detectable from the two separate graphs for  $\rho_s$  and  $\rho_v$ .

The results in Fig. 8 are closer to those for the reference sample than the data for the unpolished samples in Fig. 5. This can be easily explained in that the polishing treatment removes the layer with the greatest concentration of silver and/or titania, which are responsible of the analyzed properties: the only samples that exhibits higher values than the reference sample, even after polishing, are the samples treated with solutions at lower concentrations. This confirms that these solutions are able to penetrate deeper, influencing  $\rho_v$  more than  $\rho_s$ . Obviously, Ag solutions produce a more marked effect.

The results obtained show that the best performance as an antistatic material is achieved using less concentrated solutions that penetrate deeper into the ceramic substrate and enhance the different effects on volume and surface resistivity, with a strong improvement of the  $\chi$  values, resulting in a material that discharges to ground rather than to surface.

#### 4. Conclusions

The surface functionalization of industrial ceramic tiles was successfully obtained by the addition of soluble salts. Mechanical properties (scratch and wear resistance) and conductivity were both improved using titanium and silver solutions while maintaining the aesthetic appearance of the finished product. The results obtained show that scratch resistance generally increases with the addition of titanium soluble salts. On the contrary, addition of silver does not affect mechanical properties, which are thus mainly influenced by the Ti content. However, addi-

tion of silver strongly decreases volume resistivity without a significant variation in surface resistivity, providing good anti-static properties. In particular, the effect of soluble silver salt is strongly linked to the dilution of the solutions: the best anti-static performance is obtained with the lowest Ag concentration solution.

#### Acknowledgements

Support from the Prin2007 project, “Made in Italy in the ceramic industry for building use. Nanopowders and nanotechnologies for aesthetic innovation and functionalization of ceramic surfaces”, (20073MZALE) and experimental help from Dr. Alessandro Ferrari and Dr. Gianluca Maini are gratefully acknowledged.

#### References

- Watson GS, Watson JA. Natural nano-structures on insects—possible functions of ordered arrays characterized by atomic force microscopy. *Appl Surf Sci* 2004;**235**:139.
- Wang R, Hashimoto K, Fujishima A, Chikuni M, Kojima E, Kitamura A, Shimohigoshi M, Watanabe T. Light-induced amphiphilic surfaces. *Nature* 1997;**388**:431.
- Fujishima A, Rao TN, Tryk DA. Titanium dioxide photocatalyst. *J Photochem Photobiol* 2000;**C1**:1.
- Fujishima A, Rao TN, Tryk DA. TiO<sub>2</sub> photocatalysts and diamond electrodes. *Electrochim Acta* 2000;**45**:4683.
- Benedix R, Dehn F, Quaas J, Orgass M. Application of titanium dioxide photocatalysis to create self-cleaning building materials. *Lacer* 2000;**5**:157.
- Bondioli F, Taurino R, Ferrari AM. Functionalization of ceramic tile surface by sol–gel technique. *J Colloid Sci Interface* 2009;**334**:195–201.
- Bondioli F, Manfredini T, Giorgi M, Vignali G. Functionalization of ceramic tile surface by soluble salts addition: Part I. *J Eur Ceram Soc* 2010;**30**:11–6.
- Siracusano S, Baglio V, D’Urso C, Antonucci V, Aricò AS. Preparation and characterization of titanium suboxides as conductive supports of IrO<sub>2</sub> electrocatalysts for application in SPE electrolyzers. *Electrochim Acta* 2009;**54**:6292–9299.
- Wilk GD, Wallace RM, Anthony JM. High-k gate dielectrics: current status and materials properties considerations. *J Appl Phys* 2001;**89**:5243–75.
- Oshawa A. Electrostatic characterization of antistatic floors using an equivalent circuit model. *J Electrostat* 2001;**51/52**:625–31.
- CIE, Recommendations of Uniform Color Spaces, Color Difference Equations, Psychometrics Color Terms. Supplement No. 2 of CIE Publ. no. 15 (E1-1.31) 1971, Bureau Central de la CIE, Paris; 1978.
- Hunter RS. Photoelectric color difference meter. *J Opt Soc Am* 1958;**48**:985.
- Pierson JF, Rousselot C. Stability of reactively sputtered silver oxide films. *Surf Coat Technol* 2005;**200**:276–9.
- [www.crct.polymtl.ca/fact/documentation/TDNUcl/Ag-O.jpg](http://www.crct.polymtl.ca/fact/documentation/TDNUcl/Ag-O.jpg).
- [www.goodfellow.com](http://www.goodfellow.com).